A Coordinated Frequency Regulation Framework Based on Hybrid Battery-Ultracapacitor Energy Storage Technologies

UMER AKRAM [ID], (Student Member, IEEE), AND MUHAMMAD KHALID, (Member, IEEE)

Electrical Engineering Department, King Fahd University of Petroleum and Minerals, Dhahran 31261, Saudi Arabia

Corresponding author: Umer Akram (g201512930@kfupm.edu.sa)

ABSTRACT The replacement of conventional electricity generators by wind turbines and solar photovoltaic panels results in reduced system inertia, which jeopardizes the electric power system frequency. Frequency variation is critical as it may cause equipment damage and blackouts. Frequency regulation (FR) plays a crucial role in sustaining the stability of electric power grids by minimizing the instantaneous mismatches between electric power generation and load demand. Regulation service (RS) providers dynamically inject/absorb electric power to/from the grid, in response to regulation signals provided by independent system operators (ISOs), in order to keep the frequency within the permissible limits. The regulation signals are highly transient and hence require quick responding resources in order to provide FR effectively. This paper proposes innovative design and operation frameworks for state-of-the-art battery-energy storage system (BESS) and ultracapacitor (UC)-based hybrid energy storage system (HESS) employed for FR in electricity market. The proposed system design framework is based upon the initial investment cost, replacement cost, maintenance cost, and financial penalty imposed by ISO on RS provider for not supplying the required RS. The proposed system operation framework allocates power to both BESS and UC based upon their maximum power ratings while fulfilling their constraints at the same time. The frequent partial charge–discharge transitions, which are detrimental for BESS, are reduced by using two battery banks instead of one large battery bank. The charging and discharging of two battery banks are controlled innovatively to reduce the transitions between the partial charge–discharge transitions. Moreover, a comparison based upon cost per unit between two cases, that is: 1) HESS employed for FR and 2) BESS employed for FR, is presented, which shows that the HESS is more economical.

INDEX TERMS Frequency regulation, hybrid energy storage, battery, supercapacitor, optimization.

I. INTRODUCTION

During the past few decades, rising concerns for global warming and volatile fossil fuels prices have made renewable energy (RE) sources an attractive alternative. This trend has been further underpinned by rapid advancements in the power electronics field [1], [2], which enabled full controllability of RE sources, within the constraints inflicted by the natural phenomenon [3]. Since, such sources are intermittent, uncontrollable, stochastic, and highly variable, their integration in the electric power grid poses challenges to its effective operation, especially at higher penetration levels [4]. For example, load mismatch, poor load following, voltage instability, frequency deviation, inferior power quality, and reliability problems are some of the detrimental impacts that

RE sources introduce in electric power network [5], [6]. The large scale integration of RE sources in the power system reduces the system inertia, which results in significant decline in frequency control [7]–[9].

Electric power system is required to maintain the frequency within the acceptable range, for its stable and reliable operation. Frequency regulation (FR) can be attained by precisely matching the power generation and load demand. FR has three levels, namely primary, secondary, and tertiary regulation [10]. The primary FR requires action from regulation source within few seconds when the system frequency falls outside the non-critical frequency window, to quickly restore the balance between the generated active power and load power demand. Due to the stringent requirement on the

response time, primary FR is the most expensive regulation reserve. This is because traditionally the primary FR is performed by thermal generators, which are designed to commit bulk load, but not as quick response reserves. To complement the generation side FR, load side FR has been considered as a techno-economical alternative [11], [12]. Nevertheless, load side FR is constrained by end use disutility caused by load curtailment [13].

Independent system operators (ISOs) that manage and operate electric power grids are liable for FR. Multiple ISOs, e.g., Cal-ISO in California, ERCOT in Texas, NYISO in New York, PJM across multiple states in the eastern U.S., MSA in Alberta, IESO in Ontario, AEMO in Australia, and New England ISO in England provide market-based FR. In a regulation service (RS) market operated by an ISO, RS resources counter the detrimental effects caused by change in generation/demand for stable and reliable operation of electric power grid. RS providers are paid for dynamically supplying/consuming electric power to/from the electric power grid, in response to the regulation signals provided by the ISOs. It is predicted in a report that the total revenue from the RS market would be between $20 – $57 billion by 2022 [14].

The FR is a hard task in conventional power grids as load demand is not impeccably predictable and power generation plants have limited ramp up/down capabilities. In modern power grid paradigm the FR task has become even more challenging due to the integration of RE sources which adds unpredictability to the generation. Moreover, RE share in the power system is expected to increase, and this leads to an increase in required capacity for FR. Thus, novel techniques for procuring and settling FR are necessary. The current mechanisms are unreasonable and inordinately discriminatory against faster ramping resources that are clearly required to meet future FR needs, especially at the higher penetration levels of RE sources. Furthermore, the use of faster ramping resources for FR has the potential to enhance techno-economic efficiency of the electric power grid [15].

Energy storage systems are considered as the promising RS resources to provide regulation services [16], [17]. Several types of energy storage systems are available and among them battery energy storage systems (BESSs) are most frequently utilized as the BESSs have faster response time as compared to the conventional generators [18]–[20]. Moreover, contemporary regulatory developments [21] require ISOs to pay extra incentives to expeditiouly responding RS resources, promoting the usage of BESSs in regulation markets. Batteries are only efficient at responding to steady fluctuation, while regulation signals are highly fluctuating, which are not suitable for them. It is difficult for batteries to recover from rapid power swings without a significant reduction in their lifetime [22]. Moreover, the profit achievable by deploying BESS is generally limited because of their limited cycle life, since BESS replacement cost can greatly diminish profits.

An ideal energy storage system must have a high power density to follow rapid power fluctuations, a high energy density to give autonomy to the RS provider, and longer life to maximize the profit [23]. As a sole energy storage technology is unlikely to deliver these essentials effectively and economically, it is vital to couple multifarious energy storage technologies, creating a hybrid energy storage system (HESS). For example, BESS and ultracapacitor/supercapacitor (UC) technology can be coupled to build HESS. The BESSs have high specific energy, low specific power, low self-discharge, low cycle life, long charge times, higher cost per watt, and relatively lower cost per watt-hour. On the other hand, the UC storage systems have high specific power, low specific energy, high cycle life, very high self-discharge, short charge times, lower cost per watt, and higher cost per watt-hour [24], [25]. The HESS makes use of complementary properties of BESS and UC and provides large energy supply, high power, and fast dynamic response at the same time economically and effectively [26]–[29]. Nevertheless, to optimize the lifetime of both BESS and UC, it is vital to ensure that both operate within their operational constraints. BESS must operate within its state-of-charge (SOC) and current bounds and UC within its voltage and current bounds. At the same time the UC should respond to rapid high current signals in order to maximize the lifespan of the BESS [30]. Therefore, in order to maximize the profit it is crucial for a RS provider to optimize both capacity and operation of HESS.

In literature different strategies have been presented for FR. These studies have been carried out either considering a generic BESS [31], [32] or focusing on a specific energy storage technology like lead acid batteries [33], Li-ion batteries [34], [35], vanadium redox flow batteries [36], flywheels [37], or super conducting magnetic energy storage [38].

In [31], a methodology for the sizing of energy storage system in terms of power and energy capacities has been developed to provide the FR. The proposed technique has been applied to a 12-bus grid model with high wind power penetration. The estimated storage size for inertial response and primary FR services has been validated through real time simulations. In [39], the combination of BESS and UC technology has deployed for smoothing of wind power. High pass and low pass filters have been used to supply the steady fluctuations to BESS and rapid fluctuations to UC. In [40], a probabilistic approach has been used to size the energy storage for FR of a system having high solar penetration. To meet a certain frequency response, number of simulations with many different storage sizes has been performed in [41] and a relation between the storage capacity and frequency deviation has been derived for the studied system. A control scheme for a storage system providing FR in microgrids has been proposed in [42]. In [43], a fixed-frequency sliding-mode-controlled boost-inverter based BESS-UC has been proposed. The sliding mode controller has been designed using variable amplitude PWM carrier signals. The sliding mode controller has used to allocate the power to BESS and UC system. Various other control techniques have also been developed to control the BESS-UC HESSs, such as model
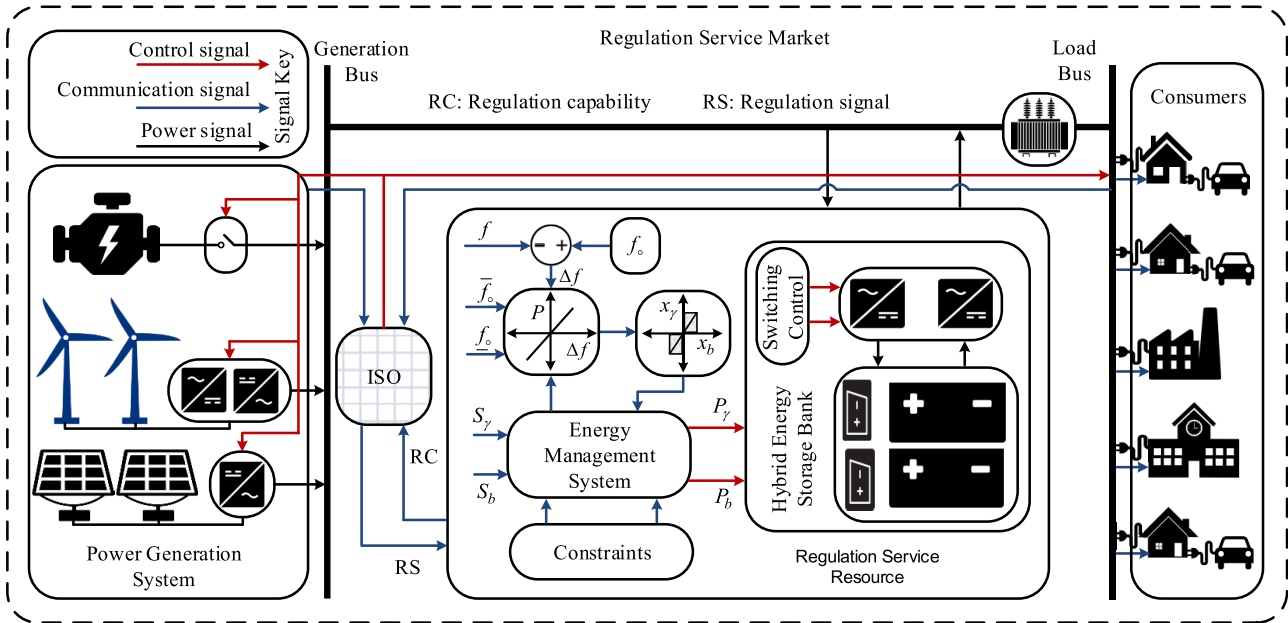
FIGURE 1. Electricity regulation market.

predictive control, rule-based control, neural networks, and fuzzy logic control [30], [44], [45]. In [46], a methodology has been developed to allocate the energy required for FR to each storage unit within multi-storage units with the aim of ameliorating system reliability. It has been presented through case studies that the required power is more effectively distributed by using the proposed methodology and thus the method alleviates more frequency fluctuation, as compared to the conventional method. In [47], a power sharing methodology based upon a combination of Haar wavelet transform and fuzzy logic control has been proposed for energy management system of the hybrid tramway employing fuel cell, BESS, and UC hybrid storage. In [48], a control strategy based upon low-pass filter and fuzzy logic controller has been proposed for hybrid BESS-UC system. First the low-pass filter removes the highly fluctuating components from the signal supplied to BESS. The fuzzy logic controller minimizes the BESS peak current while constantly considering the state-of-charge of the UC.

In this paper, a design framework is developed for the HESS employed by a RS provider to provide FR in electricity market paradigm. The design framework is based upon the total expenditure of RS provider, compensation paid by ISO, and the penalty imposed ISO for not supplying required regulation. Moreover, a novel operation framework is also developed for the operation of HESS. The proposed operation framework allocates the power to BESS and UC based upon their maximum power ratings. The proposed operation strategy does not lose any small piece of information sent by ISO via regulation signal which is a drawback in filter based techniques. In addition, an innovative operation strategy for BESS is also developed to overcome the frequent partial charge-discharge transitions problem of BESS in HESS.

As a case study, a real world frequency measurement signal is used to test the proposed methodology. Simulation results depict the effectiveness of the proposed approach.

The remainder of the paper is organized as follows. Section II presents system design framework. System operation framework is given in Section III. Simulation results and discussions are given in Section IV and Section V concludes the paper.

II. SYSTEM DESIGN FRAMEWORK

Fig. 1 illustrates the simplified operation of electricity regulatory market. The RS provider submits its regulation capability to ISO that it can supply during a period of operation. After accepting the offer ISO sends a regulation signal to the RS provider. The RS provider dynamically injects/absorbs power to/from the system in response to the regulation signal. The RS provider is paid at the end of the operation based upon the total energy supplied and absorbed.

We define $M = \{0, 1, \ldots, 11\}$ be the set containing months numbers, $D = \{0, 1, \ldots, 29\}$ denotes days within a month, $H = \{0, 1, \ldots, 23\}$, denotes the hours within a day, and $\tau = \{0, \Delta t, 6\Delta t, \ldots, 600\Delta t\}$ represents the time with a step of 6 seconds within a hour. The entire year is indexed by taking cross product $(m, d, h, t) \in M \times D \times H \times \tau$. The inter-month, inter-day and inter-hour transition follow $(m, d + 29, d, t) = (m + 1, 0, h, t)$, $(m, d, h + 23, t) = (m, d + 1, 0, t)$, and $(m, d, h, t + 600\Delta t) = (m, d, h + 1, 0)$ respectively. For the purpose of brevity the indexes m, d, and h are removed.

Let $F^t = (S_\alpha^t, S_\beta^t, S_\gamma^t, R^t, P^t, G^t)$ be the state of the system at time t. S_α^t and S_β^t are the SOC of the battery banks. In this study, we have assumed two battery banks instead of single large BESS in order to reduce the frequent partial charge-

discharge transitions. This novel charge-discharge concept is explained in detail in the next section. S_γ^t is the energy stored in UC. P^t is the cost of the energy at time t in $/MWh and G^t models the financial penalty, which is the opposite of measurement of how well HESS tracks the regulation signal. In this study, we assume that P^t is fixed doing so will not affect the results as in this case it has been assumed that RS provider has already cleared the bidding process. R^t is the regulation signal translated in terms of power. We assume that ISO send system frequency as a regulation signal. The power deficit (power that causing frequency deviation) and system frequency can be approximated by linear relation. R^t is modeled as follows

$$R^t = \kappa \left[\mathbf{1}_{\{f^t > \overline{f_o}\}}(f^t - \overline{f_o}) - \mathbf{1}_{\{f^t < \underline{f_o}\}}(\underline{f_o} - f^t) \right] \quad (1)$$

where $\mathbf{1}_{\{\star\}}$ is the indicator function, κ is the constant, f^t is the system frequency and it is updated after every 6 seconds, $\overline{f_o}$ in the upper limit of allowable frequency deviation, and $\underline{f_o}$ is the lower limit of allowable frequency deviation. It can be observed from (1) that when frequency goes above the allowable frequency deviation then $R^t > 0$, which means HESS absorbs power from the system and starts charging, $R^t < 0$ means discharging of HESS, and $R^t = 0$ represents idle mode (no charging/discharging).

At every time t our system decision is $x^t = (x_\alpha^t, x_\beta^t, x_\gamma^t)$. x_α^t, x_β^t are the responses in MW from battery banks and x_γ^t is the response in MW from the UC based upon the regulation signal provided by ISO which changes after every 6 seconds. $x^t > 0$ means charging of HESS, $x^t < 0$ means discharging of HESS, and $x^t = 0$ represents idle mode(no charging/discharging). When output of HESS perfectly follows the regulation signal then $|R^t + x_\alpha^t + x_\beta^t + x_\gamma^t| = 0$. At every time t battery banks and UC should also remain within their specified state-of-charge limits.

$$S_\alpha^{min} \leq S_\alpha^t + x_\alpha^t \leq S_\alpha^{max} \quad (2)$$
$$S_\beta^{min} \leq S_\beta^t + x_\beta^t \leq S_\beta^{max} \quad (3)$$
$$S_\gamma^{min} \leq S_\gamma^t + x_\gamma^t \leq S_\gamma^{max} \quad (4)$$

where S_α^{max}, S_β^{max}, and S_γ^{max} are the maximum energy storage capacities of the battery banks and UC. Similarly, at every time t charged/discharged power should also be within the maximum power ratings.

$$|x_\alpha^t| \leq P_\alpha^{max} \quad (5)$$
$$|x_\beta^t| \leq P_\beta^{max} \quad (6)$$
$$|x_\gamma^t| \leq P_\gamma^{max} \quad (7)$$

where P_α^{max}, P_β^{max}, and P_γ^{max} are the maximum power capacities of battery banks and UC. If RS provider fails to follow the regulation signal, ISO penalizes the RS provider. Mathematically, the financial penalty is modeled as following

$$G^t = \upsilon \left(\mathbf{1}_{\{R^t + x_\alpha^t + x_\beta^t + x_\gamma^t = 0\}} |R^t + x_\alpha^t + x_\beta^t + x_\gamma^t| \right) \hat{t}$$
$$+ \upsilon \left(\mathbf{1}_{\{R^t + x_\alpha^t + x_\beta^t + x_\gamma^t \neq 0\}} |R^t + x_\alpha^t + x_\beta^t + x_\gamma^t| \right) \hat{t} \quad (8)$$

where υ is the penalty in $/MWh, $|R^t + x_\alpha^t + x_\beta^t + x_\gamma^t|$ is the power (MW) not supplied or taken from the system, and $\hat{t}$ is time step in hour. In this study υ is kept fixed throughout the operation of RS provider.

Let $F^{t+\Delta t} = S^M(F^t, x^{t+\Delta t})$ be the mapping of system states from t to $t + \Delta t$. The change in the level of stored energy at $t + \Delta t$ is modeled as given below

$$S_\alpha^{t+\Delta t} = S_\alpha^t + x_\alpha^{t+\Delta t} \left(\mathbf{1}_{\{x_\alpha^{t+\Delta t} > 0\}}\eta^c + \mathbf{1}_{\{x_\alpha^{t+\Delta t} < 0\}}\frac{1}{\eta^d} \right) \hat{t} \quad (9)$$

$$S_\beta^{t+\Delta t} = S_\beta^t + x_\beta^{t+\Delta t} \left(\mathbf{1}_{\{x_\beta^{t+\Delta t} > 0\}}\eta^c + \mathbf{1}_{\{x_\beta^{t+\Delta t} < 0\}}\frac{1}{\eta^d} \right) \hat{t} \quad (10)$$

$$S_\gamma^{t+\Delta t} = S_\gamma^t + x_\gamma^{t+\Delta t} \left(\mathbf{1}_{\{x_\gamma^{t+\Delta t} > 0\}}\eta + \mathbf{1}_{\{x_\gamma^{t+\Delta t} < 0\}}\eta \right) \hat{t} \quad (11)$$

where η^c, is the charging efficiency of battery, η^d is the discharging efficiency of battery, and η is the charging/discharging efficiency of UC. η^c, η^d, and η accounts the loss in energy during conversion. It is important to note that same type of batteries are employed in both battery banks that is why same values of charging and discharging efficiency are used in (9) and (10).

The BESS and UC have limited number of life cycles. So, for realistic analysis it is crucial to consider BESS and UC cycles. We assume that the life of BESS and UC depend upon the life cycles and after completing their life cycles BESS and UC are replaced. The lifetimes of BESS and UC are calculated using the following equations

$$T_\alpha = \sum_{m=0}^{11} \sum_{d=0}^{29} \sum_{h=0}^{23} \sum_{t=0}^{600\Delta t} \lfloor \frac{x_\alpha^{m,d,h,t}}{2S_\alpha^{max}} \rceil \quad (12)$$

$$T_\beta = \sum_{m=0}^{11} \sum_{d=0}^{29} \sum_{h=0}^{23} \sum_{t=0}^{600\Delta t} \lfloor \frac{x_\beta^{m,d,h,t}}{2S_\beta^{max}} \rceil \quad (13)$$

$$T_\gamma = \sum_{m=0}^{11} \sum_{d=0}^{29} \sum_{h=0}^{23} \sum_{t=0}^{600\Delta t} \lfloor \frac{x_\gamma^{m,d,h,t}}{2S_\gamma^{max}} \rceil \quad (14)$$

where T_α, T_β, and T_γ are life of battery banks and UC in years. The total compensation paid by the ISO to RS provider for providing the regulation service for one year is calculated as

$$C_T = \sum_{m=0}^{11} \sum_{d=0}^{29} \sum_{h=0}^{23} \sum_{t=0}^{600\Delta t} P^{m,d,h,t} \left[x_\gamma^{m,d,h,t} \left(\mathbf{1}_{\{x_\gamma^{m,d,h,t} > 0\}}\eta \right. \right.$$
$$\left. \left. - \mathbf{1}_{\{x_\gamma^{m,d,h,t} < 0\}}\eta \right) \right]$$
$$+ \sum_{m=0}^{11} \sum_{d=0}^{29} \sum_{h=0}^{23} \sum_{t=0}^{600\Delta t} P^{m,d,h,t} \left[x_\alpha^{m,d,h,t} \left(\mathbf{1}_{\{x_\alpha^{m,d,h,t} > 0\}}\eta^c \right. \right.$$
$$\left. \left. - \mathbf{1}_{\{x_\alpha^{m,d,h,t} < 0\}}\frac{1}{\eta^d} \right) \right]$$
$$+ \sum_{m=0}^{11} \sum_{d=0}^{29} \sum_{h=0}^{23} \sum_{t=0}^{600\Delta t} P^{m,d,h,t} \left[x_\beta^{m,d,h,t} \left(\mathbf{1}_{\{x_\beta^{m,d,h,t} > 0\}}\eta^c \right. \right.$$
$$\left. \left. - \mathbf{1}_{\{x_\beta^{m,d,h,t} < 0\}}\frac{1}{\eta^d} \right) \right] \quad (15)$$
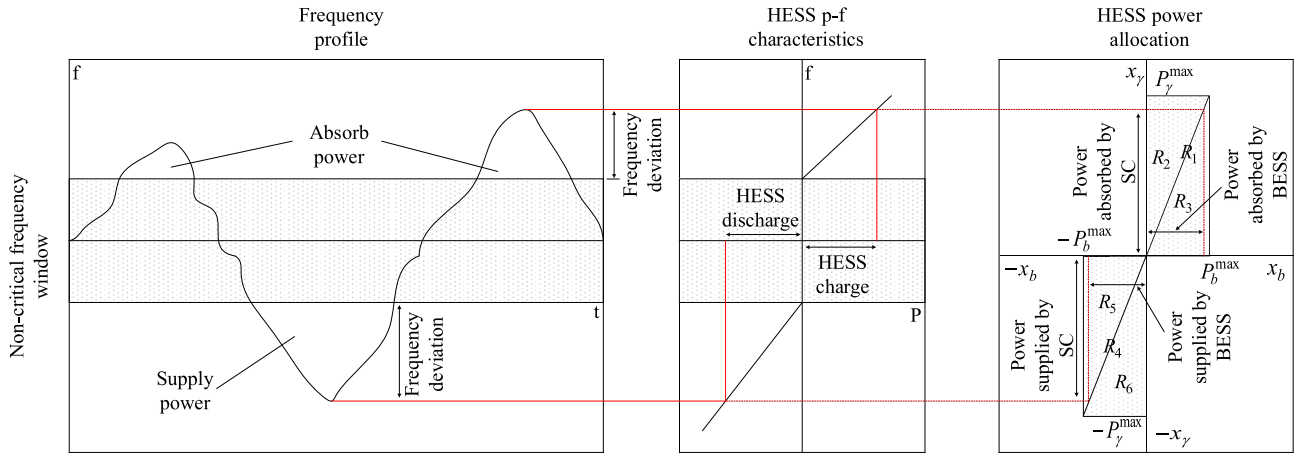
FIGURE 2. Power frequency characteristics of HESS.

where C_T is the total compensation of period of one year. Similarly, the financial penalty cost C_P of one year is calculated using the following equation

$$C_P = \sum_{m=0}^{11} \sum_{d=0}^{29} \sum_{h=0}^{23} \sum_{t=0}^{600\Delta t} G^{m,d,h,t} \tag{16}$$

In this study we assume that the RS provider participate in the regulation market for 20 years. The total expenditure of RS provider is calculated as given below

$$
\begin{aligned}
C_h &= C_\alpha^{c,e} S_\alpha^{max} + C_\alpha^{c,p} P_\alpha^{max} + C_\beta^{c,e} S_\beta^{max} + C_\beta^{c,p} P_\beta^{max} \\
&\quad + C_\gamma^{c,p} P_\gamma^{max} + C_\gamma^{c,e} S_\gamma^{max} \\
&\quad + \sum_{\ell=1}^{n_\ell} \frac{C_\alpha^{om} P_\alpha^{max} + C_\beta^{om} P_\beta^{max} + C_\gamma^{om} P_\gamma^{max}}{(1+\eth)^\ell} \\
&\quad + \sum_{l_\alpha=T_\alpha}^{n_\ell - T_\alpha} \frac{C_\alpha^{c,e} S_\alpha^{max} + C_\alpha^{c,p} P_\alpha^{max}}{(1+\eth)^{l_\alpha}} \\
&\quad + \sum_{l_\beta=T_\beta}^{n_\ell - T_\beta} \frac{C_\beta^{c,e} S_\beta^{max} + C_\beta^{c,p} P_\beta^{max}}{(1+\eth)^{l_\beta}} \\
&\quad \times \sum_{l_\gamma=T_\gamma}^{n_\ell - T_\gamma} \frac{C_\gamma^{c,e} S_\gamma^{max} + C_\gamma^{c,p} P_\gamma^{max}}{(1+\eth)^{l_\gamma}}
\end{aligned}
\tag{17}
$$

where

$$
\begin{aligned}
l_\alpha &= T_\alpha, 2T_\alpha, 3T_\alpha, \ldots, n_\ell - T_\alpha \\
l_\beta &= T_\beta, 2T_\beta, 3T_\beta, \ldots, n_\ell - T_\beta \\
l_\gamma &= T_\gamma, 2T_\gamma, 3T_\gamma, \ldots, n_\ell - T_\gamma
\end{aligned}
$$

where $C_\alpha^{c,e}$, $C_\beta^{c,e}$, and $C_\gamma^{c,e}$, are capital investment costs associated with energy capacities two battery banks and UC in $/MWh, $C_\alpha^{c,p}$, $C_\beta^{c,p}$, and $C_\gamma^{c,p}$, are capital investment costs associated with power capacities battery banks and UC in $/MW, C_α^{om}, C_β^{om}, and C_γ^{om}, are operation and maintenance costs of battery banks and UC in $/MW − yr, n_ℓ is the years

of operation, and $\eth$ is the discount rate. l_α, l_β, and l_γ are the indexes that increase with a step equal to T_α, T_β, and T_γ.

We propose the following objective function to maximize the profit of RS provider while satisfactorily providing FR.

$$obj : J = J_1(X) + J_2(X) \to \min \tag{18}$$

$$s.t. \begin{cases} g_w(X) = 0 & w = 1, 2, , \ldots, m \\ h_\iota(X) \leq 0 & \iota = 1, 2, , \ldots, q \end{cases} \tag{19}$$

where J_1 is the ratio of the total expenditure of RS provider to the compensation paid by ISO, J_2 is the total value of financial penalty imposed by ISO on RS provider, **g** and **h** are equality and inequality constraints inflicted by the operation of BESS and UC, and $X = \left[S_\alpha^{max}, S_\beta^{max}, S_\gamma^{max}, P_\alpha^{max}, P_\beta^{max}, P_\gamma^{max} \right]$ are the design variables. The techno-economic of BESS and UC is given in Table 1.

III. SYSTEM OPERATION FRAMEWORK

The operation of HESS with the change in system frequency is shown in Fig. 2. When frequency goes above the non-critical frequency window the HESS start charging in order to take the surplus power from the system casing decrease in frequency. Similarly, when frequency falls below the non-critical frequency window the HESS injects power in the system in order to supply the power deficit causing an increase in the frequency. The required power power that is needed to be injected/absorbed to/from the system is assigned to BESS and UC based upon their maximum power ratings. The graphical illustration of the power allocation algorithm is shown in Fig. 2. Let $x_b^t = x_\alpha^t + x_\beta^t$, $P_b^{max} = P_\alpha^{max} + P_\beta^{max}$, and $m = P_\gamma^{max}/P_b^{max}$. Depending upon the HESS states and constraints the power allocation algorithm operates in one of the six regions $\{R_1, R_2, R_3, R_4, R_5, R_6\}$ as shown in Fig. 2. Mathematically, the six regions bounds are

$$R_1 : \begin{cases} x_\gamma^t = mx_b^t \\ x_\gamma^t \leq P_c^{max} & \forall t > 0 \\ x_b^t \leq P_b^{max} \end{cases} \tag{20}$$

TABLE 1. Techno-economic data of BESS and UC [49].

Type	Energy capital cost($/kWh)	Power capital cost($/kW)	Operation and maintenance cost ($/KW-yr)	Life Cycles	DOD
BESS	300	1000	80	2500	100%
UC	500	200	80	100000	100%

$$R_2 : \begin{cases} x_\gamma^t > mx_b^t \\ x_\gamma^t \leq P_\gamma^{max} \quad \forall t > 0 \\ x_b^t > P_b^{max} \end{cases} \tag{21}$$

$$R_3 : \begin{cases} x_\gamma^t < mx_b^t \\ x_\gamma^t < P_\gamma^{max} \quad \forall t > 0 \\ x_b^t \leq P_b^{max} \end{cases} \tag{22}$$

$$R_4 : \begin{cases} x_\gamma^t = mx_b^t \\ x_\gamma^t \geq -P_\gamma^{max} \quad \forall t > 0 \\ x_b^t \geq -P_b^{max} \end{cases} \tag{23}$$

$$R_5 : \begin{cases} x_\gamma^t > mx_b^t \\ x_\gamma^t > -P_\gamma^{max} \quad \forall t > 0 \\ x_b^t \geq -P_b^{max} \end{cases} \tag{24}$$

$$R_6 : \begin{cases} x_\gamma^t = mx_b^t \\ x_\gamma^t \geq -P_\gamma^{max} \quad \forall t > 0 \\ x_b^t > -P_b^{max} \end{cases} \tag{25}$$

We define the following two conditions

$$C1 : \text{if } x_b^t > P_b^{max} \text{ then } x_b^t = P_b^{max}$$
$$C2 : \text{if } x_\gamma^t > P_\gamma^{max} \text{ then } x_\gamma^t = P_\gamma^{max}$$

These two conditions **C1** and **C2** make sure that both BESS and UC operate within their maximum power rating capacities. The power allocation to BESS and UC is done using the following seven rules.

$$\Gamma_1 : \text{if } R^{t+\Delta t}$$
$$> 0 \text{ and } S_b^t + \hat{t}x_b^{t+\Delta t} \leq S_b^{max} \text{ and } S_\gamma^t + \hat{t}x_\gamma^{t+\Delta t}$$
$$\leq S_\gamma^{max} \text{ then } x_b^{t+\Delta t} = \frac{R^{t+\Delta t}}{m+1} \text{ and } x_\gamma^{t+\Delta t} = mx_b^{t+\Delta t} \tag{26}$$

$$\Gamma_2 : \text{if } R^{t+\Delta t}$$
$$> 0 \text{ and } S_b^t + \hat{t}x_b^{t+\Delta t} > S_b^{max} \text{ and } S_\gamma^t + \hat{t}x_\gamma^{t+\Delta t}$$
$$\leq S_\gamma^{max} \text{ then } x_b^{t+\Delta t} = \frac{S_b^{max} - S_b^t}{\hat{t}} \text{ and } x_\gamma^{t+\Delta t}$$
$$= R^{t+\Delta t} - x_b^{t+\Delta t} \tag{27}$$

$$\Gamma_3 : \text{if } R^{t+\Delta t}$$
$$> 0 \text{ and } S_b^t + \hat{t}x_b^{t+\Delta t} \leq S_b^{max} \text{ and } S_\gamma^t + \hat{t}x_\gamma^{t+\Delta t}$$
$$> S_\gamma^{max} \text{ then } x_\gamma^{t+\Delta t} = \frac{S_\gamma^{max} - S_\gamma^t}{\hat{t}} \text{ and } x_b^{t+\Delta t}$$
$$= R^{t+\Delta t} - x_\gamma^{t+\Delta t} \tag{28}$$

$$\Gamma_4 : \text{if } R^{t+\Delta t}$$
$$< 0 \text{ and } S_b^t + \hat{t}x_b^{t+\Delta t} \geq S_b^{min} \text{ and } S_\gamma^t + \hat{t}x_\gamma^{t+\Delta t}$$
$$< S_\gamma^{min} \text{ then } x_\gamma^{t+\Delta t} = \frac{S_\gamma^t - S_\gamma^{min}}{\hat{t}} \text{ and } x_b^{t+\Delta t}$$
$$= R^{t+\Delta t} - x_\gamma^{t+\Delta t} \tag{29}$$

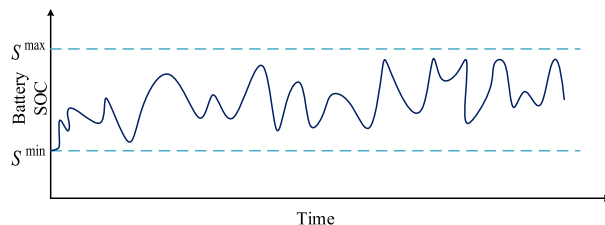**FIGURE 3.** Conventional charging/discharging of BESS.

$$\Gamma_5 : \text{if } R^{t+\Delta t}$$
$$< 0 \text{ and } S_b^t + \hat{t}x_b^{t+\Delta t} < S_b^{min} \text{ and } S_\gamma^t + \hat{t}x_\gamma^{t+\Delta t}$$
$$\geq S_\gamma^{min} \text{ then } x_b^{t+\Delta t} = \frac{S_b^t - S_b^{min}}{\hat{t}} \text{ and } x_\gamma^{t+\Delta t}$$
$$= R^{t+\Delta t} - x_b^{t+\Delta t} \tag{30}$$

$$\Gamma_6 : \text{if } R^{t+\Delta t}$$
$$< 0 \text{ and } S_b^t + \hat{t}x_b^{t+\Delta t} \geq S_b^{min} \text{ and } S_\gamma^t + \hat{t}x_\gamma^{t+\Delta t}$$
$$\geq S_\gamma^{min} \text{ then } x_b^{t+\Delta t} = \frac{R^{t+\Delta t}}{m+1} \text{ and } x_\gamma^{t+\Delta t}$$
$$= mx_b^{t+\Delta t} \tag{31}$$

$$\Gamma_7 : \text{if } R^{t+\Delta t}$$
$$= 0 \text{ then } x_b^{t+\Delta t} = 0 \text{ and } x_\gamma^{t+\Delta t} = 0 \tag{32}$$

The conditions $C1$ and $C2$ are necessary conditions for $\Gamma_i \, \forall i = 1, 2, \ldots, 7$. So, $\Gamma_i \Rightarrow C1$ and $\Gamma_i \Rightarrow C2 \, \forall i = 1, 2, \ldots, 7$. Only one rule can be true at a time. The solution for every rule is bounded by the six regions, i.e., the solution of Γ_i is bounded by $R_i \, \forall i = 1, 2, \ldots, 6$. For Γ_7 only one solution possible i.e., $x_b^{t+\Delta t} = 0$ and $x_\gamma^{t+\Delta t} = 0$. From the above discussion it can be observed that, in R_1 and R_4 power allocation to BESS and UC is done using $x_b^t = R^t / (m+1)$ and $x_\gamma^t = mx_b^t$ respectively. The proposed power allocation algorithm operates in R_3 and R_5 when UC does not has enough energy to fulfill power allocation relation given above. Similarly, the proposed algorithm operates in R_2 and R_6 when BESS does not has enough energy to fulfill power allocation relation. It is important to note that the BESS and UC constraints will always be fulfilled. It can be observed that the proposed power allocation algorithm uses all the information supplied by the regulation, and even a small piece of information is not lost.

The highly transient nature of the regulation signal implies that the BESS undergoes very frequent, albeit partial, charge and discharge cycles as shown in Fig. 3. As such, battery degradation is a major practical problem faced by BESS based RS systems [14], [50]. In order to overcome this problem we propose an innovative charge-discharge strategy which substantially reduces the charge/discharge transitions as shown in Fig. 4. The BESS is assumed to be consist
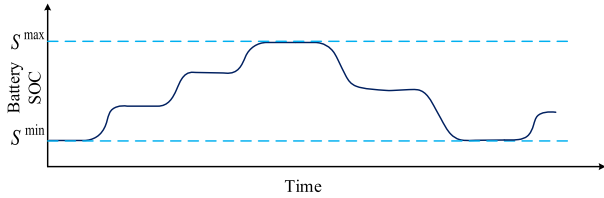
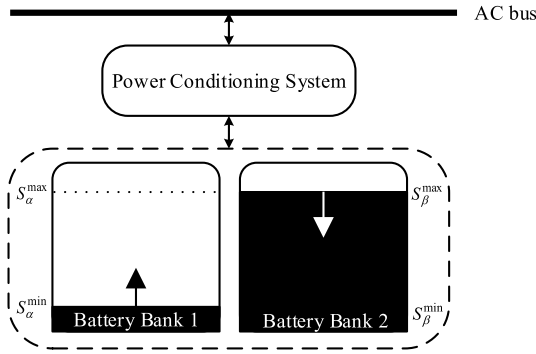**FIGURE 4.** Proposed charging/discharging of BESS.

FIGURE 5. Structure of BESS for proposed charge/discharge scheme.

charging/discharging scheme is as follows

$$if\ S_\alpha^t = 0\ and\ S_\alpha^{t-\Delta t} > 0\ then\ v_\alpha = U^+ and\ v_\beta = U^-$$
$$if\ S_\alpha^t = S_\alpha^{max}\ and\ S_\alpha^{t-\Delta t} < S_\alpha^{max}\ then\ v_\alpha = U^-$$
$$and\ v_\beta = U^+$$
$$if\ S_\beta^t = 0\ and\ S_\beta^{t-\Delta t} > 0\ then\ v_\beta = U^+ and\ v_\alpha = U^-$$
$$if\ S_\beta^t = S_\beta^{max}\ and\ S_\beta^{t-\Delta t} < S_\beta^{max}\ then\ v_\beta = U^-$$
$$and\ v_\alpha = U^+$$

In other words, the battery banks changes their charge/discharge status when one of them reaches its lower or upper specified limit of its storage capacity.

IV. SIMULATION RESULTS AND DISCUSSIONS

The proposed methodology is tested by using the real frequency measurements from an electric power grid. The data has a resolution of 6 seconds. The exact name and location of the power grid is not mentioned due to the confidentiality. The frequency signal of real world electric power grid is shown in Fig. 6. The non-critical frequency window is set between 49.95Hz – 50.05Hz. The fluctuations that are within
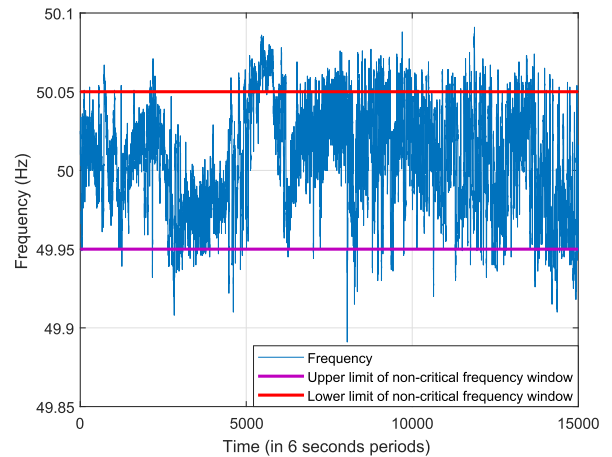
of two battery banks, one battery bank charges and other discharges as shown in Fig. 5. The battery bank which is charging keeps on charging until it reach its maximum capacity and afterwards it starts discharging to its minimum allowable value and starts charging again and so on. Consider the BESS shown in Fig. 5 consists of two battery banks whose maximum energy capacities are S_α^{max} and S_β^{max} and maximum power capacities are P_α^{max} and P_β^{max}. It is assumed that each individual battery bank is charged/discharged independently by utilizing its own power converter which allows their autonomous control. The exploration of power converter topologies and their control is beyond the scope of this study. The number of power converters coupled with each battery banks may be increased by choosing the autonomous control strategy which result in an increase in cost of the system which is always a concern for every engineering design, but there are number of benefits associated with this type of control. For example, 1) increased redundancy and availability, e.g., if one power converter malfunctions the other can still supply the power and support the system which is not possible with only one converter, 2) cost and benefits can always be weighed against each other and the proposed scheme has several benefits against traditional solutions, and 3) life of batteries can be increased and their aging can be delayed due to proposed scheme.

Let v_α and v_β are the symbolic variables that show the status of the two battery banks by taking a value in the set of two symbols $\{U^+, U^-\}$. $v_\alpha = U^+$ and $v_\beta = U^+$ shows charging and $v_\alpha = U^-$ and $v_\beta = U^-$ shows discharging. v_α and v_β can take the values using the two rules, i.e., $v_\alpha = U^+$ iff $v_\beta = U^-$ and $v_\alpha = U^-$ iff $v_\beta = U^+$. Initially, we set $v_\alpha = U^+$ and $v_\beta = U^-$. The proposed
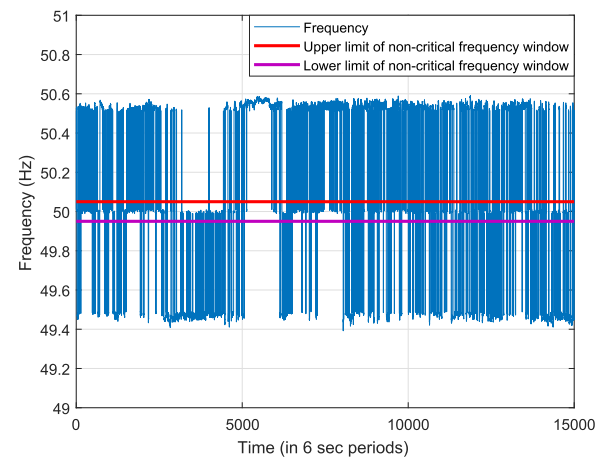

FIGURE 6. Real world frequency signal.

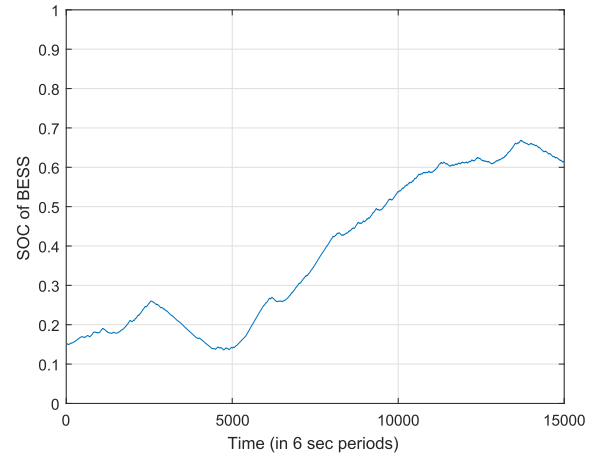**FIGURE 7.** System frequency (regulation signal).

the non-critical frequency window are considered as normal and require no counter actions. To include the impact of RE sources the frequency signal is modified such that 10% of the frequency value is added to the fluctuations that are above 50.01Hz and 10% of frequency value is subtracted from the fluctuations that are below 49.99Hz. The modified frequency signal is shown in Fig. 7. We assume that ISO sends the modified frequency signal shown in Fig. 7 to RS provider.

The optimal size of energy storage system is characterized by both energy storing capacity and maximum power rating. The energy (MWh) and power (MW) capacities of BESS and UC determined, using the system design framework proposed in Section II, are tabulated in Table 2. These capacities are used to provide FR, and the power allocation algorithm proposed in Section III is used to operate the HESS. To regulate the frequency with in the permissible bounds the RS provider continuously injects/absorbs power in the system in response to the regulation signal. The regulated frequency is shown in Fig. 8. It can be observed that the frequency is effectively regulated and it is within the non-critical window. All the events for which frequency deviates from the non-critical window the RS provider regulates them by charging/discharging the HESS appropriately, RS provider takes no action during the instants for which frequency is within the non-critical window.

TABLE 2. Optimal capacities of BESS and UC.

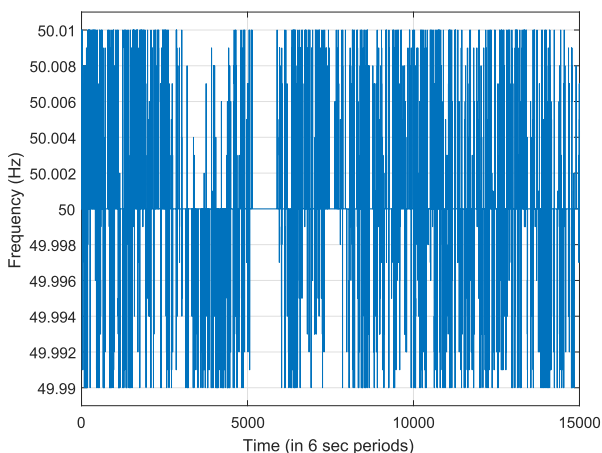| BESS (MWh)	BESS (MW)	UC (MWh)	UC (MW)
97	8.8	2	6

As mentioned earlier that one of the primary purposes to utilize BESS-UC coupled system is to increase the life of BESS by keeping its charge/discharge rate steady. The variation in SOC of BESS and UC corresponding to the regulation signal (Fig. 7) are shown in Fig. 9 and Fig. 10 respectively. It can be observed that SOC of BESS changes
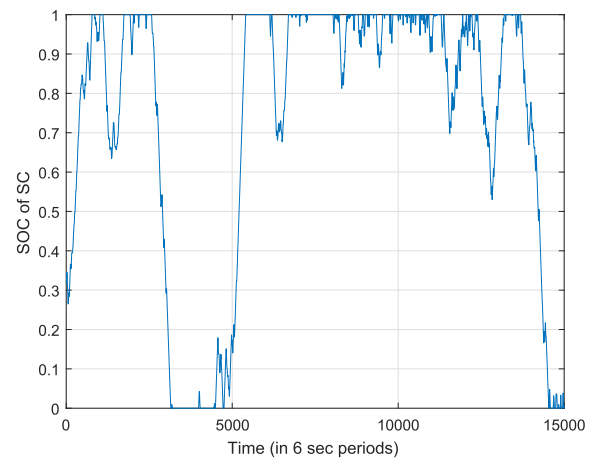
FIGURE 8. Regulated frequency of the system.

FIGURE 9. SOC of BESS.

FIGURE 10. SOC of SC.

gradually which is desired, while SOC of UC fluctuates between minimum and maximum value.

The variation in the SOC of HESS along with the change in the system frequency is shown in Fig. 11. It can be observed that whenever frequency goes above 50.05Hz which is the upper limit of non-critical frequency window, the HESS absorbs power from the system to regulate the frequency which results in an increase in SOC of HESS. Similarly, when frequency of the system goes below 49.95Hz which is the lower limit of non-critical frequency window, the HESS injects the power in the system to regulate the frequency which results in a decrease in SOC of HESS. It can also be observed that during the instants when frequency deviation is within the non-critical frequency window HESS does not inject or absorb the power and SOC of HESS remains constant during such instants. So, from the above results and discussion its is evident that the proposed methodology efficiently distributes the power between BESS and UC and effectively regulates the frequency within the required limits.

As explained in Section III that in this study we assumed more than one battery banks each having independent
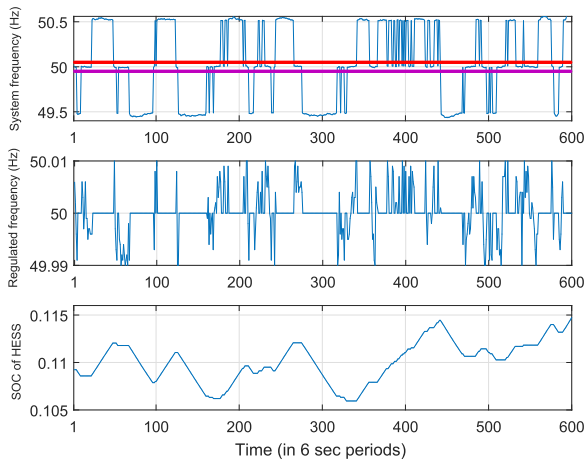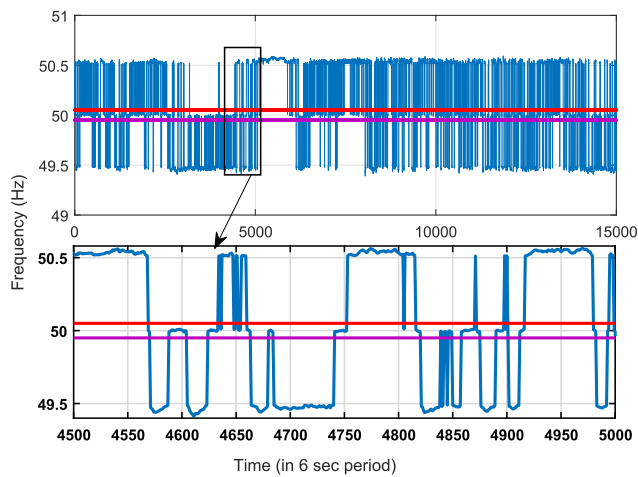
FIGURE 11. SOC of HESS vs system frequency.

FIGURE 12. System frequency.

FIGURE 13. Charging/discharging of BESS using proposed charge/discharge scheme.

charge/discharge control instead of a single battery bank in order to avoid frequent partial charge-discharge transitions. The variation in system frequency and corresponding variation in SOC of two battery banks are shown in Fig. 12 and Fig. 13 respectively. When system frequency falls below the non-critical frequency window the battery bank which is discharging injects power in the grid and results in a decrease in SOC of this battery bank. The battery bank which is charging remains in idle mode and its SOC remains constant. Similarly, when the system frequency goes above the non-critical frequency window that battery bank which is charging starts taking power from the system thereby increasing its SOC. The battery bank which is discharging remains in idle state during this period. The battery banks exchange the charging/discharging states whenever anyone of them reaches to its minimum or maximum stored energy limits.

The proposed design and operation frameworks are also used for the capacity optimization and operation of BESS employed for FR. The cost per unit for HESS and BESS are calculated. It has been found that the per-unit cost of BESS is 10.4% more as compared to HESS. This increase in cost due to fact that in HESS the UC improves the battery life which
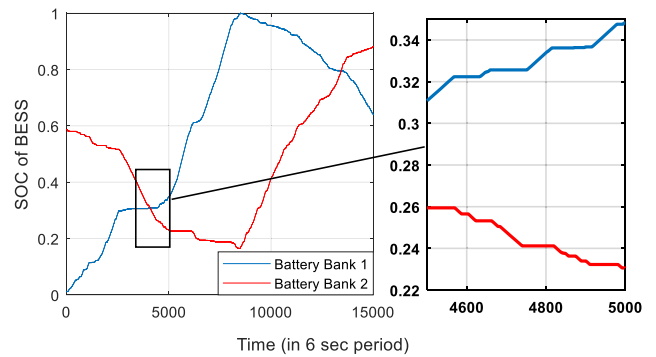
results in reduction in replacement cost battery. It is important to note that this increase in cost is in one unit and RS provider supplies large amount of energy. Hence, by installing HESS instead of BESS a RS providers can save substantial amount of money. Moreover, the response time of HESS is small as compared to BESS which results in better FR performance.

V. CONCLUSION

In this paper, an innovative design framework has been proposed for hybrid energy storage system (coupled BESS and UC) followed by an efficient coordinated operation scheme to regulate system frequency in electricity markets particularly in response to higher penetration of renewable power into electricity grids. The design framework takes into account different associated costs such as initial investment cost, operation and maintenance cost, replacement cost, and financial penalty imposed by ISO for not supplying required regulation. The operation framework is developed in such a way that it allocates power automatically to BESS and UC based upon their maximum power ratings while fulfilling their operational constraints. Furthermore, a novel operation strategy for BESS has also been proposed to avoid frequent and partial charge and discharge transitions so as to prolong the life of the BESS. It was proved through simulations that the proposed coordinated framework is capable of ensuring proper frequency regulation without losing any small piece of information, which can be a problem in filter-based techniques. The significance of the scheme lies in the fact that a RS provider can save a substantial amount of money by employing HESS instead of BESS alone to provide primary frequency regulation in power system operation.

REFERENCES

[1] O. Ellabban, H. Abu-Rub, and F. Blaabjerg, "Renewable energy resources: Current status, future prospects and their enabling technology," *Renew. Sustain. Energy Rev.*, vol. 39, pp. 748–764, Nov. 2014.

[2] J. M. Carrasco *et al.*, "Power-electronic systems for the grid integration of renewable energy sources: A survey," *IEEE Trans. Ind. Electron.*, vol. 53, no. 4, pp. 1002–1016, 2006.

[3] F. Blaabjerg, R. Teodorescu, M. Liserre, and A. V. Timbus, "Overview of control and grid synchronization for distributed power generation systems," *IEEE Trans. Ind. Electron.*, vol. 53, no. 5, pp. 1398–1409, Oct. 2006.

[4] J. Zhu *et al.*, "Learning automata-based methodology for optimal allocation of renewable distributed generation considering network reconfiguration," *IEEE Access*, vol. 5, pp. 14275–14288, 2017.

[5] A. Kyritsis *et al.*, "Evolution of PV systems in Greece and review of applicable solutions for higher penetration levels," *Renew. Energy*, vol. 109, pp. 487–499, Aug. 2017.

[6] U. Akram, M. Khalid, and S. Shafiq, "Optimal sizing of a wind/solar/battery hybrid grid-connected microgrid system," *IET Renew. Power Generat.*, vol. 12, no. 1, pp. 72–80, 2017.

[7] E. Ela, A. Tuohy, M. Milligan, B. Kirby, and D. Brooks, "Alternative approaches for incentivizing the frequency responsive reserve ancillary service," *Elect. J.*, vol. 25, no. 4, pp. 88–102, 2012.

[8] J. Eto, "Use of frequency response metrics to assess the planning and operating requirements for reliable integration of variable renewable generation," Lawrence Berkeley Nat. Lab., Berkeley, CA, USA, LBNL Paper LBNL-4142E, 2011. [Online]. Available: http://escholarship.org/uc/item/0kt109pn

[9] S. Sharma, S.-H. Huang, and N. Sarma, "System inertial frequency response estimation and impact of renewable resources in ERCOT interconnection," in *Proc. Power Energy Soc. General Meeting*, Jul. 2011, pp. 1–6.

[10] P. Kundur, N. J. Balu, and M. G. Lauby, *Power System Stability and Control*, vol. 7. New York, NY, USA: McGraw-Hill, 1994.

[11] C. Zhao, U. Topcu, and S. H. Low, "Optimal load control via frequency measurement and neighborhood area communication," *IEEE Trans. Power Syst.*, vol. 28, no. 4, pp. 3576–3587, Nov. 2013.

[12] C. Zhao, U. Topcu, N. Li, and S. Low, "Design and stability of load-side primary frequency control in power systems," *IEEE Trans. Autom. Control*, vol. 59, no. 5, pp. 1177–1189, May 2014.

[13] Y. J. Zhang, C. Zhao, W. Tang and S. H. Low, "Profit maximizing planning and control of battery energy storage systems for primary frequency control," *IEEE Trans. Smart Grid*, 2016, doi: 10.1109/TSG.2016.2562672.

[14] Y. Kim, V. Raghunathan, and A. Raghunathan, "Design and management of battery-supercapacitor hybrid electrical energy storage systems for regulation services," *IEEE Trans. Multi-Scale Comput. Syst.*, vol. 3, no. 1, pp. 12–24, Jan. 2017.

[15] A. D. Papalexopoulos and P. E. Andrianesis, "Performance-based pricing of frequency regulation in electricity markets," *IEEE Trans. Power Syst.*, vol. 29, no. 1, pp. 441–449, Jan. 2014.

[16] B. J. Kirby, *Frequency Regulation Basics and Trends*. New York, NY, USA: United States Department Energy, 2005.

[17] A. Khatamianfar, M. Khalid, A. V. Savkin, and V. G. Agelidis, "Improving wind farm dispatch in the australian electricity market with battery energy storage using model predictive control," *IEEE Trans. Sustain. Energy*, vol. 4, no. 3, pp. 745–755, Jul. 2013.

[18] Q. Zhai, K. Meng, Z. Y. Dong, and J. Ma, "Modeling and analysis of lithium battery operations in spot and frequency regulation service markets in Australia electricity market," *IEEE Trans. Ind. Informat.*, vol. 13, no. 5, pp. 2576–2586, Oct. 2017.

[19] M. Khalid and A. V. Savkin, "A model predictive control approach to the problem of wind power smoothing with controlled battery storage," *Renew. Energy*, vol. 35, no. 7, pp. 1520–1526, 2010.

[20] A. V. Savkin, M. Khalid, and V. G. Agelidis, "A constrained monotonic charging/discharging strategy for optimal capacity of battery energy storage supporting wind farms," *IEEE Trans. Sustain. Energy*, vol. 7, no. 3, pp. 1224–1231, Mar. 2016.

[21] K. Kumaraswamy and J. Cotrone, "Evaluating the regulation market maturity for energy storage devices," *Electr. J.*, vol. 26, no. 10, pp. 75–83, 2013.

[22] T. Ma, H. Yang, and L. Lu, "Development of hybrid battery-supercapacitor energy storage for remote area renewable energy systems," *Appl. Energy*, vol. 153, pp. 56–62, Sep. 2015.

[23] U. Akram, M. Khalid, and S. Shafiq, "An innovative hybrid wind-solar and battery-supercapacitor microgrid system—Development and optimization," *IEEE Access*, vol. 5, pp. 25897–25912, 2017.

[24] A. Schneuwly, "High reliability power backup with advanced energy storage," Maxwell Technol. San Diego, CA, USA, White Paper, 2006, accessed: Nov. 11, 2017. [Online] https://www.tecategroup.com/whitepapers/200904_WhitePaper_EDNEurope_ASchneuwly.pdf

[25] Q. Xu *et al.*, "A decentralized dynamic power sharing strategy for hybrid energy storage system in autonomous DC microgrid," *IEEE Trans. Ind. Electron.*, vol. 64, no. 7, pp. 5930–5941, Jul. 2017.

[26] J. Shen and A. Khaligh, "A supervisory energy management control strategy in a battery/ultracapacitor hybrid energy storage system," *IEEE Trans. Transport. Electrific.*, vol. 1, no. 3, pp. 223–231, Oct. 2015.

[27] Y. Liu, W. Du, L. Xiao, H. Wang, S. Bu, and J. Cao, "Sizing a hybrid energy storage system for maintaining power balance of an isolated system with high penetration of wind generation," *IEEE Trans. Power Syst.*, vol. 31, no. 4, pp. 3267–3275, Jul. 2016.

[28] S. Zhang, R. Xiong, and J. Cao, "Battery durability and longevity based power management for plug-in hybrid electric vehicle with hybrid energy storage system," *Appl. Energy*, vol. 179, pp. 316–328, Oct. 2016.

[29] J. M. Blanes and R. Gutiérrez, A. Garrigós, J. L. Lizán, and J. M. Cuadrado, "Electric vehicle battery life extension using ultracapacitors and an FPGA controlled interleaved buck–boost converter," *IEEE Trans. Power Electron.*, vol. 28, no. 12, pp. 5940–5948, Dec. 2013.

[30] B. Hredzak, V. G. Agelidis, and M. Jang, "A model predictive control system for a hybrid battery-ultracapacitor power source," *IEEE Trans. Power Electron.*, vol. 29, no. 3, pp. 1469–1479, Mar. 2014.

[31] V. Knap, S. K. Chaudhary, D.-I. Stroe, M. Swierczynski, B.-I. Craciun, and R. Teodorescu, "Sizing of an energy storage system for grid inertial response and primary frequency reserve," *IEEE Trans. Power Syst.*, vol. 31, no. 5, pp. 3447–3456, Sep. 2016.

[32] R. Hollinger, L. M. Diazgranados, F. Braam, T. Erge, G. Bopp, and B. Engel, "Distributed solar battery systems providing primary control reserve," *IET Renew. Power Generat.*, vol. 10, no. 1, pp. 63–70, 2016.

[33] A. Oudalov, D. Chartouni, and C. Ohler, "Optimizing a battery energy storage system for primary frequency control," *IEEE Trans. Power Syst.*, vol. 22, no. 3, pp. 1259–1266, Aug. 2007.

[34] M. Świerczyński *et al.*, "Field experience from Li-Ion BESS delivering primary frequency regulation in the Danish energy market," *ECS Trans.*, vol. 61, no. 37, pp. 1–14, 2014.

[35] D. Fooladivanda, C. Rosenberg, and S. Garg, "Energy storage and regulation: An analysis," *IEEE Trans. Smart Grid*, vol. 7, no. 4, pp. 1813–1823, Jul. 2016.

[36] A. Lucas and S. Chondrogiannis, "Smart grid energy storage controller for frequency regulation and peak shaving, using a vanadium redox flow battery," *Int. J. Elect. Power Energy Syst.*, vol. 80, pp. 26–36, Sep. 2016.

[37] K. Vidyanandan and N. Senroy, "Frequency regulation in a wind–diesel powered microgrid using flywheels and fuel cells," *IET Generat., Transmiss. Distrib.*, vol. 10, no. 3, pp. 780–788, 2016.

[38] J. Li, R. Xiong, Q. Yang, F. Liang, M. Zhang, and W. Yuan, "Design/test of a hybrid energy storage system for primary frequency control using a dynamic droop method in an isolated microgrid power system," *Appl. Energy*, vol. 201, pp. 257–269, Sep. 2017.

[39] L. Bai, F. Li, Q. Hu, H. Cui, and X. Fang, "Application of battery-supercapacitor energy storage system for smoothing wind power output: An optimal coordinated control strategy," in *Proc. Power Energy Soc. General Meeting (PESGM)*, 2016, pp. 1–5.

[40] M. Yue and X. Wang, "Grid inertial response-based probabilistic determination of energy storage system capacity under high solar penetration," *IEEE Trans. Sustain. Energy*, vol. 6, no. 3, pp. 1039–1049, Jul. 2015.

[41] T. Masuta and A. Yokoyama, "Supplementary load frequency control by use of a number of both electric vehicles and heat pump water heaters," *IEEE Trans. Smart Grid*, vol. 3, no. 3, pp. 1253–1262, Sep. 2012.

[42] I. Serban and C. Marinescu, "Control strategy of three–phase battery energy storage systems for frequency support in microgrids and with uninterrupted supply of local loads," *IEEE Trans. Power Electron.*, vol. 29, no. 9, pp. 5010–5020, Sep. 2014.

[43] D. B. W. Abeywardana, B. Hredzak, and V. G. Agelidis, "A fixed-frequency sliding mode controller for a boost-inverter-based battery-supercapacitor hybrid energy storage system," *IEEE Trans. Power Electron.*, vol. 32, no. 1, pp. 668–680, Jan. 2017.

[44] J. Moreno, M. E. Ortúzar, and J. W. Dixon, "Energy-management system for a hybrid electric vehicle, using ultracapacitors and neural networks," *IEEE Trans. Ind. Electron.*, vol. 53, no. 2, pp. 614–623, Apr. 2006.

[45] M. Zandi, A. Payman, J.-P. Martin, S. Pierfederici, B. Davat, and F. Meibody-Tabar, "Energy management of a fuel cell/supercapacitor/battery power source for electric vehicular applications," *IEEE Trans. Veh. Technol.*, vol. 60, no. 2, pp. 433–443, Feb. 2011.

[46] W.-W. Kim, J.-S. Shin, and J.-O. Kim, "Operation strategy of multi-energy storage system for ancillary service," *IEEE Trans. Power Syst.*, vol. 32, no. 6, pp. 4409–4417, Nov. 2017.

[47] Q. Li, W. Chen, Z. Liu, M. Li, and L. Ma, "Development of energy management system based on a power sharing strategy for a fuel cell-battery-supercapacitor hybrid tramway," *J. Power Sources*, vol. 279, pp. 267–280, Apr. 2015.

[48] L. W. Chong, Y. W. Wong, R. K. Rajkumar, and D. Isa, "An optimal control strategy for standalone PV system with battery-supercapacitor hybrid energy storage system," *J. Power Sources*, vol. 331, pp. 553–565, Nov. 2016.

[49] X. Luo, J. Wang, M. Dooner, and J. Clarke, "Overview of current development in electrical energy storage technologies and the application potential in power system operation," *Appl. Energy*, vol. 137, pp. 511–536, Jan. 2015.

[50] S. B. Peterson, J. Apt, and J. F. Whitacre, "Lithium-ion battery cell degradation resulting from realistic vehicle and vehicle-to-grid utilization," *J. Power Sources*, vol. 195, no. 8, pp. 2385–2392, 2010.

UMER AKRAM (S'16) received the B.Sc. degree (Hons.) in electrical engineering from the COM-SATS Institute of Information Technology, Abbottabad, Pakistan, in 2013. He is currently pursuing the M.S. degree in electrical engineering from the King Fahd University of Petroleum and Minerals, Dhahran, Saudi Arabia. His current research interests include modern power system planning, operation and design, the optimization and control of distributed energy resources, renewable energy, and energy storage systems.

MUHAMMAD KHALID (M'09) received the Ph.D. degree in electrical engineering from the School of Electrical Engineering and Telecommunications (EE&T), University of New South Wales (UNSW), Sydney, Australia, in 2011. He was a Post-Doctoral Research Fellow for three years and then a Senior Research Associate with the School of EE&T, Australian Energy Research Institute, UNSW, for another two years. He is currently an Assistant Professor with the Electrical Engineering Department, King Fahd University of Petroleum and Minerals, Dhahran, Saudi Arabia. He has authored/co-authored several journals and conference papers in the field of control and optimization for renewable power systems. His current research interests include the optimization and control of battery energy storage systems for large-scale grid-connected renewable power plants (particularly wind and solar), distributed power generation and dispatch, hybrid energy storage, EVs, and smart grids. In addition, he has been a reviewer for numerous international journals and conferences. He was a recipient of a highly competitive Post-Doctoral Writing Fellowship from UNSW in 2010.

• • •